Template Synthesis, Structure and Characterization of $Ni^{II}{}_2Pb^{II}$ and $Cu^{II}{}_2Pb^{II}$ Complexes of Macrocycles with a N_4O_2 Donor Set†

Makoto Tadokoro, Hisashi Ōkawa,* Naohide Matsumoto, Masayuki Koikawa and Sigeo Kida
Department of Chemistry, Faculty of Science, Kyushu University, Hakozaki, Higashiku, Fukuoka 812, Japan

The reaction of [*N,N'*-ethylene- or [*N,N'*-propane-1,3-diylbis(3-formyl-5-methylsalicylideneiminato)]-metal(II) (M = Cu or Ni) and a diamine (ethylenediamine, propane-1,3-diamine, butane-1,4-diamine or pentane-1,5-diamine) in the presence of lead(II) ion gives macrocyclic complexes $[Pb(ML^{m,n})_2]X_2$ [$H_2L^{m,n}$ = macrocycle formed by the condensation of two molecules of 2,6-diformyl-4-methylphenol and two diamines $H_2N(CH_2)_mNH_2$ and $H_2N(CH_2)_nNH_2$; $m = 2$ or 3 and $n = 2$–5; M = Cu or Ni; X = ClO_4, PF_6, BPh_4 or BF_4]. They were characterized by elemental analyses, single-crystal X-ray analysis, fast atom bombardment mass, IR, electronic and ESR spectra and magnetic measurements. The crystal structure of $[Pb(CuL^{3,3})_2][ClO_4]_2$ has revealed that the copper(II) ion in each $CuL^{3,3}$ is bound at one of the N_2O_2 donor sites and the lead ion is sandwiched by the vacant N_2O_2 sites of two $CuL^{3,3}$ entities, providing a square-antiprismatic environment.

The chemistry of macrocyclic binuclear complexes has been stimulated by a desire to mimic the active sites of some metalloenzymes,[1] to search appropriate systems for binding and activating small molecules,[2] and to investigate the mutual influence of two metal centres on the electronic, magnetic and redox properties of such systems.[2–4] Pilkington and Robson[5] first reported the 'direct' template synthesis of a binucleating macrocycle comprised of two molecules of 2,6-diformyl-4-methylphenol and two molecules of propane-1,3-diamine [Fig. 1(*a*), $m = n = 3$; the macrocycles of this type are abbreviated as $L^{m,n}$ hereafter]. We[6] reported the 'stepwise' template synthesis of the macrocycles $L^{2,2}$, $L^{2,3}$ and $L^{3,3}$. Those and related macrocycles have been extensively used for studies on homo- and hetero-binuclear complexes and mixed-valence complexes.[7–12] Recently, an analogue with fully reduced azomethine linkages [Fig. 1(*b*)] was obtained for $m = n = 3$ and its binuclear copper(II) complexes were electrochemically and structurally studied.[13] It is suggested that the saturation of the azomethine linkages has a significant effect upon the stereochemistry and redox properties of the dicopper(II) complexes. However, fully saturated macrocyclic analogues are unknown except for that of $m = n = 3$.

Our aim in this study was to establish an efficient synthetic method of the unreduced macrocycles with various combinations of *m* and *n* [Fig. 1(*a*)], because the direct template reaction of Pilkington and Robson[5] is only applicable for macrocycles of the same alkane chains ($m = n$) and our stepwise template reaction gave only poor results for the synthesis of the macrocycles with longer alkane chains [$m(n) > 3$]. The present work is essential for our further purpose to develop the co-ordination chemistry of homo- and hetero-binuclear complexes using the macrocyclic analogues reduced at the azomethine linkages [Fig. 1(*b*)]. In this study we have obtained macrocycles $L^{2,3}$, $L^{2,4}$, $L^{2,5}$, $L^{3,3}$ and $L^{3,4}$ as $Ni^{II}{}_2Pb^{II}$ or $Cu^{II}{}_2Pb^{II}$ complexes of general formula $[Pb(ML^{m,n})_2]X_2$ (M = Ni or Cu; X = ClO_4, PF_6, BPh_4 or BF_4). One complex, $[Pb(CuL^{3,3})_2][ClO_4]_2$, was structurally analysed by single-crystal X-ray crystallography.

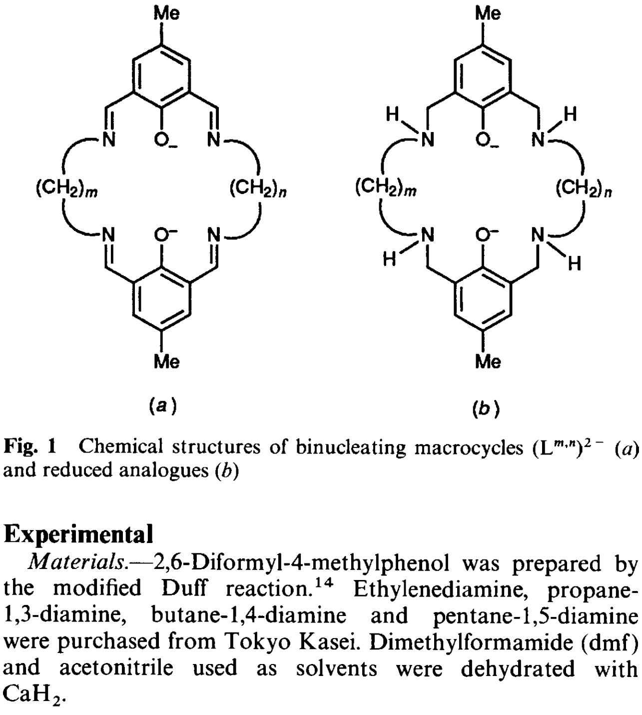

Fig. 1 Chemical structures of binucleating macrocycles $(L^{m,n})^{2-}$ (*a*) and reduced analogues (*b*)

Experimental

Materials.—2,6-Diformyl-4-methylphenol was prepared by the modified Duff reaction.[14] Ethylenediamine, propane-1,3-diamine, butane-1,4-diamine and pentane-1,5-diamine were purchased from Tokyo Kasei. Dimethylformamide (dmf) and acetonitrile used as solvents were dehydrated with CaH_2.

Syntheses.—[*N,N'*-Ethylenebis(3-formyl-5-methylsalicylideneiminato)]-nickel(II) and -copper(II) and *N,N'*-propane-1,3-diylbis(3-formyl-5-methylsalicylideneiminato)-nickel(II) and -copper(II) were synthesised by the literature methods.[6]

$[Pb(NiL^{2,3})_2][ClO_4]_2{\cdot}2H_2O$ **1**. A suspension of [*N,N'*-ethylenebis(3-formyl-5-methylsalicylideneiminato)]nickel(II) (2.50 g, 6.1 mmol) in dmf (40 cm^3) was mixed with a dmf solution (20 cm^3) of lead(II) perchlorate trihydrate (1.41 g, 3.1 mmol) and the mixture was refluxed with stirring. To the hot mixture was added a dmf solution (20 cm^3) of propane-1,3-diamine (0.45 g, 6.1 mmol) to form a clear orange solution, from which yellowish orange microcrystals separated within 30 min. They were recrystallized from acetonitrile.

$[Pb(NiL^{2,3})_2][PF_6]_2$ **2**. A mixture of [*N,N'*-ethylenebis(3-formyl-5-methylsalicylideneiminato)]nickel(II) (1.0 g), lead(II) acetate trihydrate (0.46 g), and ammonium hexafluoro-

---

† *Supplementary data available:* see Instructions for Authors, *J. Chem. Soc., Dalton Trans.*, 1991, Issue 1, pp. xviii–xxii.
Non-SI unit employed: G = 10^{-4} T.

Table 1 Analytical data for $[Pb(ML^{m,n})_2]X_2$ complexes

		Analysis (%)*			
Complex	Yield (%)	C	H	N	M
1 $[Pb(NiL^{2,3})_2][ClO_4]_2\cdot 2H_2O$	82	40.90	3.65	8.30	8.8
		(41.35)	(3.90)	(8.40)	(9.0)
2 $[Pb(NiL^{2,3})_2][PF_6]_2$	71	39.35	3.50	7.95	8.5
		(39.70)	(3.50)	(8.05)	(8.4)
3 $[Pb(NiL^{2,3})_2][BPh_4]_2\cdot MeCN\cdot H_2O$	50	64.30	5.30	6.85	6.4
		(64.10)	(5.20)	(7.00)	(6.5)
4 $[Pb(NiL^{2,4})_2][ClO_4]_2\cdot H_2O$	57	42.65	4.00	8.25	8.7
		(42.80)	(4.05)	(8.30)	(8.7)
5 $[Pb(NiL^{2,4})_2][PF_6]_2$	41	40.35	3.70	8.00	8.7
		(40.60)	(3.70)	(7.90)	(8.3)
6 $[Pb(NiL^{2,4})_2][BF_4]_2\cdot H_2O$	55	43.70	4.10	8.35	9.6
		(43.65)	(4.10)	(8.50)	(8.9)
7 $[Pb(CuL^{2,3})_2][ClO_4]_2$	63	41.85	3.70	8.50	9.9
		(42.15)	(3.70)	(8.55)	(9.7)
8 $[Pb(CuL^{2,4})_2][ClO_4]_2$	77	42.70	4.00	8.20	9.0
		(43.10)	(3.90)	(8.35)	(9.5)
9 $[Pb(CuL^{2,5})_2][ClO_4]_2$	55	43.60	4.20	8.10	8.9
		(43.95)	(4.15)	(8.20)	(9.3)
10 $[Pb(CuL^{3,3})_2][ClO_4]_2\cdot dmf$	88	43.15	4.35	8.80	8.7
		(43.40)	(4.20)	(8.95)	(9.0)
11 $[Pb(CuL^{3,4})_2][BPh_4]_2$	95	64.95	5.40	6.15	6.5
		(65.20)	(5.35)	(6.20)	(7.0)

* Calculated values are given in parentheses.

phosphate (0.40 g) in dmf (40 cm^3) was stirred at the boiling temperature. To this was added a dmf solution (20 cm^3) of propane-1,3-diamine (0.18 g), and the mixture was refluxed for 30 min to form a clear reddish brown solution. The reaction mixture was concentrated to dryness, and the residue was dissolved in acetonitrile (200 cm^3). The solution was concentrated to 30 cm^3 and mixed with diethyl ether to give orange microcrystals. These were recrystallized from acetonitrile–methanol (1:3).

$[Pb(NiL^{2,3})_2][BPh_4]_2\cdot MeCN\cdot H_2O$ **3**. The synthetic method was the same as that for $[Pb(NiL^{2,3})_2][PF_6]_2$ except for the use of $NaBPh_4$ instead of ammonium hexafluorophosphate.

$[Pb(NiL^{2,4})_2][ClO_4]_2\cdot H_2O$ **4**. To a gently boiled suspension of [*N,N'*-ethylenebis(3-formyl-5-methylsalicylideneiminato)]-nickel(II) (1.00 g) in dmf (40 cm^3) were added successively a dmf solution (20 cm^3) of lead(II) perchlorate trihydrate (0.56 g) and a dmf solution (20 cm^3) of butane-1,4-diamine (0.22 g). The reddish solution was refluxed for 30 min then concentrated to dryness. The residue was triturated with acetonitrile (100 cm^3) to give orange microcystals, which were recrystallized from acetonitrile.

$[Pb(NiL^{2,4})_2][PF_6]_2$ **5**. To a gently boiled mixture of [*N,N'*-ethylenebis(3-formyl-5-methylsalicylideneiminato)]nickel(II) (1.00 g), lead(II) acetate trihydrate (0.46 g), and ammonium hexafluorophosphate (0.40 g) in dmf (60 cm^3) was added a dmf solution (20 cm^3) of butane-1,4-diamine (0.22 g) to form a clear reddish solution. The reaction mixture was concentrated to dryness, and the residue dissolved in acetonitrile (400 cm^3). The solution was concentrated to 30 cm^3, mixed with ether (10 cm^3), and left to stand in a refrigerator to give orange microcrystals. These were recrystallized from methanol–dmf (9:1 v/v).

$[Pb(NiL^{2,4})_2][BF_4]_2\cdot H_2O$ **6**. This complex was obtained as reddish orange crystals in the same way as that for $[Pb(NiL^{2,4})_2][PF_6]_2$ except for the use of sodium tetrafluoroborate instead of ammonium hexafluorophosphate. It was recrystallized by dissolving in a hot acetonitrile–dmf (1:1 v/v) and then diffusing with a large amount of methanol.

$[Pb(CuL^{2,3})_2][ClO_4]_2$ **7**. A suspension of [*N,N'*-ethylenebis(3-formyl-5-methylsalicylideneiminato)]copper(II) (1.00 g) in dmf (40 cm^3) was stirred at the boiling temperature, and to this were added successively powdered lead(II) perchlorate trihydrate (0.56 g) and a dmf solution (40 cm^3) of propane-1,3-diamine (0.18 g). The resulting clear greenish brown solution was concentrated to 10 cm^3, diluted with acetonitrile (50 cm^3) and ether (20 cm^3), and allowed to stand in a refrigerator to give brown microcrystals. These were recrystallized from methanol–acetonitrile (1:1 v/v).

$[Pb(CuL^{2,4})_2][ClO_4]_2$ **8**. The synthetic method was the same as that for complex **7** except for the use of butane-1,4-diamine instead of propane-1,3-diamine. The complex was recrystallized from dmf–methanol (1:1 v/v).

$[Pb(CuL^{2,5})_2][ClO_4]_2$ **9**. A suspension of [*N,N'*-ethylenebis(3-formyl-5-methylsalicylideneiminato)]copper(II) (1.0 g) in dmf (20 cm^3) was stirred at 70 °C. To this were added a solution of lead(II) perchlorate trihydrate (0.56 g) in dmf (30 cm^3) and a solution of pentane-1,5-diamine (0.25 g) in dmf (20 cm^3) to form a clear brown solution. After stirring for 1 h at room temperature the reaction mixture was concentrated to dryness. The residue was triturated with acetonitrile (20 cm^3) to give brown microcrystals, which were recrystallized from dmf–ethanol (1:1 v/v).

$[Pb(CuL^{3,3})_2][ClO_4]_2\cdot dmf$ **10**. To a suspension of [*N,N'*-propane-1,3-diylbis(3-formyl-5-methylsalicylideneiminato)]-copper(II) (1.00 g) in dichloromethane (30 cm^3) was added an acetonitrile solution (10 cm^3) of lead(II) perchlorate trihydrate (0.54 g) to form a clear green solution. The addition of a dichloromethane solution of propane-1,3-diamine (0.17 g) resulted in the precipitation of a brown crystalline powder. This was crystallized as green prisms from methanol–dmf (1:1 v/v).

$[Pb(CuL^{3,4})_2][BPh_4]_2$ **11**. To a suspension of [*N,N'*-propane-1,3-diylbis(3-formyl-5-methylsalicylideneiminato)]-copper(II) (1.00 g) in methanol (30 cm^3) was added a solution of lead(II) acetate trihydrate (0.44 g) in hot dmf (5 cm^3), and the mixture stirred at room temperature for 10 min. Then a solution of butane-1,4-diamine (0.21 g) in methanol (20 cm^3) was added and the mixture stirred at room temperature for 30 min. The addition of a methanol solution (20 cm^3) of sodium tetraphenylborate (0.8 g) resulted in the precipitation of brown microcrystals, which were washed successively with methanol and ether, and dried in air.

Analytical results are summarized in Table 1.

Crystal Structural Analysis of $[Pb(CuL^{3,3})_2][ClO_4]_2\cdot dmf$ **10**.—Reflection data were measured on a Rigaku Denki AFC-5

Table 2 Atomic coordinates of non-hydrogen atoms (× 10^4) of $[Pb(CuL^{3,3})_2][ClO_4]_2$·dmf

Atom	*x*	*y*	*z*	Atom	*x*	*y*	*z*
Pb	2570.7(9)	229.0(3)	1647.1(4)	C(26)	1980(10)	−2317(9)	3678(13)
Cu(1)	2003.7(9)	1757.5(8)	2413.2(12)	C(27)	1324(10)	−1971(9)	3452(12)
Cu(2)	1835.4(10)	−1339.0(9)	2863.2(13)	C(28)	737(7)	−1057(8)	2606(11)
O(1)	2046(5)	798(5)	2863(7)	C(29)	536(8)	−461(8)	1950(10)
O(2)	2856(5)	1535(4)	2172(7)	C(30)	−71(8)	−177(9)	1948(11)
N(1)	1110(6)	1845(6)	2554(8)	C(31)	−305(9)	390(8)	1400(11)
N(2)	2039(6)	2679(6)	1809(9)	C(32)	−983(9)	692(10)	1343(12)
N(3)	3830(6)	477(6)	2515(9)	C(33)	89(8)	694(7)	845(10)
N(4)	2865(7)	−430(6)	3379(9)	C(34)	709(7)	460(7)	859(9)
C(1)	663(8)	2360(8)	1983(12)	C(35)	922(7)	−157(7)	1411(9)
C(2)	951(9)	3065(8)	1944(12)	C(36)	1054(8)	884(8)	304(11)
C(3)	1452(8)	3085(8)	1332(12)	C(37)	1914(9)	1419(8)	−199(11)
C(4)	2580(8)	2995(7)	1862(10)	C(38)	2213(10)	1087(10)	−962(13)
C(5)	3218(7)	2698(7)	2242(9)	C(39)	2850(12)	739(10)	−625(16)
C(6)	3765(8)	3156(8)	2435(10)	C(40)	3061(10)	−451(9)	−495(12)
C(7)	4383(8)	2938(8)	2703(10)	C(41)	3169(8)	−1143(8)	−45(11)
C(8)	4933(10)	3439(9)	2920(15)	C(42)	3619(9)	−1535(9)	−373(13)
C(9)	4499(8)	2217(8)	2758(11)	C(43)	3789(9)	−2211(9)	−18(14)
C(10)	3978(8)	1736(7)	2555(10)	C(44)	4338(11)	−2584(10)	−391(16)
C(11)	3332(7)	1966(6)	2304(9)	C(45)	3483(9)	−2484(8)	671(13)
C(12)	4199(8)	996(8)	2644(11)	C(46)	3043(7)	−2102(7)	1022(10)
C(13)	4183(9)	−192(8)	2699(12)	C(47)	2870(8)	−1420(7)	663(11)
C(14)	4050(9)	−545(8)	3627(12)	C(48)	2763(9)	−2445(8)	1726(12)
C(15)	3404(8)	−918(8)	3491(12)	Cl(A)	430(2)	−2652(2)	675(3)
C(16)	2571(8)	−415(8)	4060(11)	O(A1)	−120(8)	−2247(8)	726(12)
C(17)	2018(8)	−9(7)	4153(10)	O(A2)	253(7)	−3136(7)	−100(9)
C(18)	1714(8)	−205(8)	4901(11)	O(A3)	634(7)	−3015(8)	1578(9)
C(19)	1187(9)	107(8)	5075(12)	O(A4)	915(7)	−2219(8)	483(10)
C(20)	880(10)	−110(10)	5917(14)	Cl(B)	3744(3)	−486(3)	−3124(4)
C(21)	910(8)	658(9)	4475(12)	O(B1)*	3150(9)	−803(11)	−3162(18)
C(22)	1196(9)	895(8)	3728(11)	O(B2)*	4052(13)	−72(14)	−2376(17)
C(23)	1755(8)	573(7)	3539(10)	O(B3)*	4013(11)	−566(12)	−3928(13)
C(24)	866(8)	1461(9)	3124(11)	O(B4)*	3301(18)	101(19)	−3453(28)
O(3)	2410(5)	−1076(5)	994(7)	O(B5)*	4084(19)	−1074(18)	−2509(24)
O(4)	1491(5)	−424(4)	1389(7)	O(D)	2551(6)	2919(6)	−908(8)
N(5)	2312(6)	−2231(6)	2120(9)	N(D)	3582(7)	3187(7)	−132(9)
N(6)	1253(7)	−1424(6)	2674(9)	C(D1)	2987(9)	3358(9)	−556(12)
N(7)	1654(6)	918(6)	420(8)	C(D2)	3796((9)	2463(9)	−14(12)
N(8)	2815(8)	68(7)	−142(10)	C(D3)	4071(10)	3725(10)	159(13)
C(25)	2132(10)	−2699(9)	2851(14)				

* Occupancy factors: 0.9 for O(B1) and O(B3), 0.8 for O(B2) and 0.7 for O(B4) and O(B5).

automated four-circle diffractometer with graphite-monochromatized Mo-Kα radiation at room temperature. Three standard reflections were monitored every 100 reflections and showed no systematic decrease in intensity. The reflection data were corrected for Lorentz and polarization factors. Corrections for absorption effects were made by the Furnas method.[15] Unit-cell parameters were determined from 25 reflections ($20 < 2\theta < 30°$).

Crystal data. $C_{51}H_{59}Cl_2Cu_2N_9O_{13}Pb$, $M = 1411.3$, monoclinic, space group $P2_1/c$, crystal dimensions $0.2 \times 0.3 \times 0.4$ mm, $a = 21.239(3)$, $b = 19.241(1)$, $c = 13.999(1)$ Å, $\beta = 103.47(8)°$, $U = 5563.6$ Å^3, μ(Mo-Kα) = 39.65 cm^{-1}, $D_c = 1.685$ g cm^{-3} ($Z = 4$), $F(000) = 2824$.

Scan mode θ–2θ, scan speed 2° min^{-1}, scan range $2.5 < 2\theta < 45°$, scan width $(1.2 + 0.35 \tan\theta)°$, octant measured ($+h$, $+k$, $\pm l$). Number of reflections with $|F_o| > 3\sigma(|F_o|)$ 4807, transmission factors 1.027–1.210, $R = 0.055$, $R' = 0.065$. The largest residue in the final Fourier difference synthesis was three peaks around Pb (*ca.* 1.5 e Å^{-3}).

The structure was solved by the standard heavy-atom method and refined by block-diagonal least squares, where the function minimized was $\Sigma w(|F_o| - |F_c|)^2$ where $w = 1$ for all reflections was adopted. The contributions of hydrogen atoms bound to carbon were introduced in calculated positions. These hydrogen atoms were included in the structure-factor calculation but not refined. Atomic scattering factors were taken from ref. 16. All computations were performed on a FACOM M 780 computer at the Computer Centre of Kyushu University using the UNICS III program system.[17] The final atomic coordinates are given in Table 2.

Additional material available from the Cambridge Crystallographic Data Centre comprises H-atom coordinates, thermal parameters and remaining bond lengths and angles.

Other Physical Measurements.—Elemental analyses of carbon, hydrogen and nitrogen were obtained at the Elemental Analysis Service Centre of Kyushu University. Those of copper and nickel were made on a Shimadzu Model AA-610 atomic absorption/flame emission spectrophotometer. Fast atom bombardment (FAB) mass spectra were obtained with a JEOL JMS-DX300 spectrometer, infrared spectra on a JASCO IR-810 spectrometer using KBr disks and electronic spectra on a Shimadzu UV-210 spectrometer. Magnetic susceptibilities were measured by the Faraday method.

Results and Discussion

Preparations.—In general, success in template synthesis of macrocyclic complexes depends upon the choice of template metal ion.[18] In the previous template syntheses of $L^{m,n}$, transition-metal ions were extensively used as templates in both direct and stepwise methods.[5–7,8c,9a] Recently, Mandal *et al.*[13] reported the template synthesis of $[Pb_2L^{3,3}][NO_3]_2$ using lead(II) ion as the template. The crystal structure of the

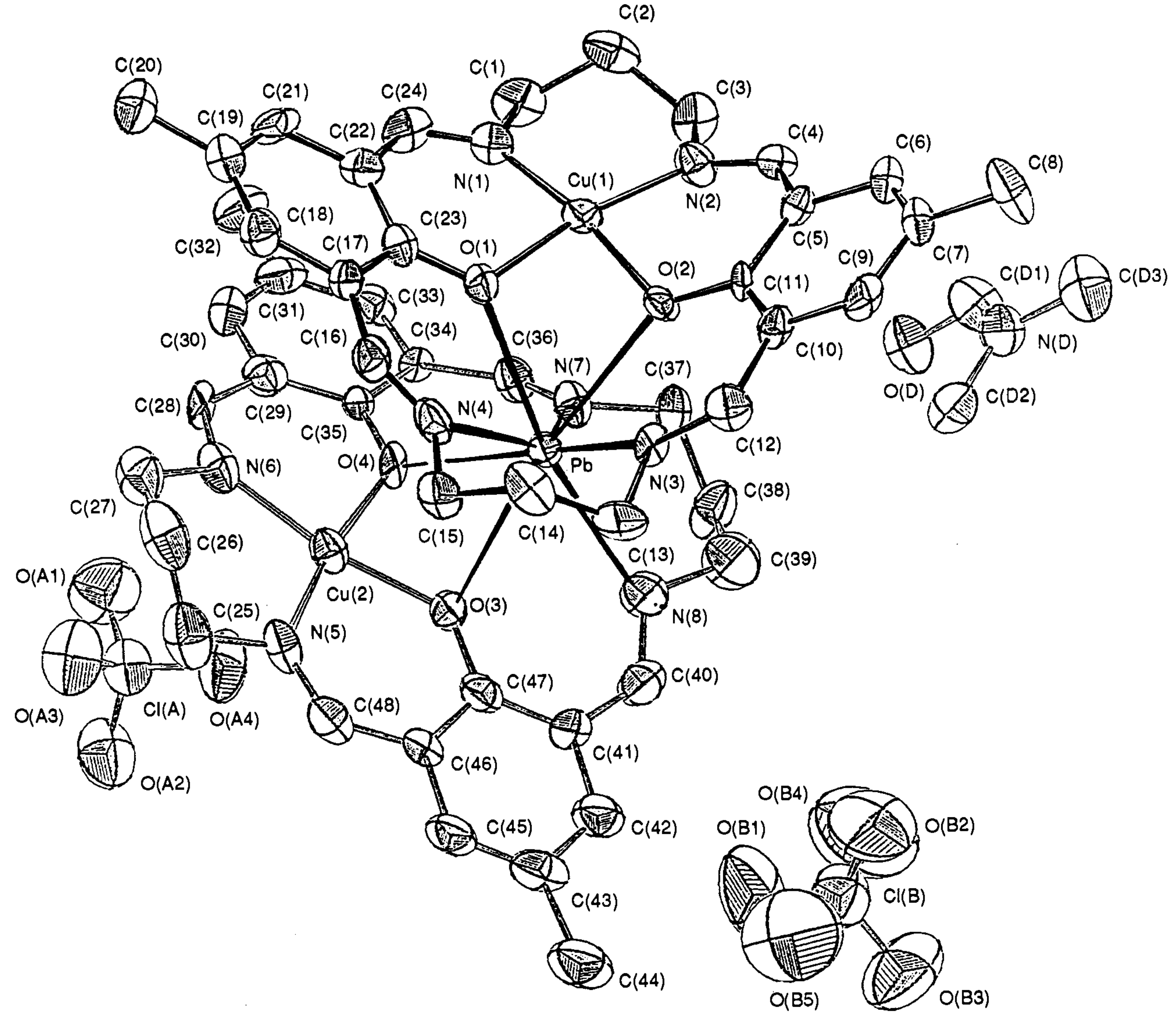

(a)

perchlorate, $[Pb_2L^{3,3}][ClO_4]_2$, was solved in our laboratory,[19] and it was found that each lead(II) ion deviates considerably from the least-squares N_2O_2 plane (1.28 Å) owing to the mismatch between the size of the co-ordination cavity and the radius of the metal ion. This result suggests a high flexibility of lead(II) ion in co-ordination. In the present case the geometrical requirement for co-ordination of the second N_2O_2 site should vary with the number (n) of methylenes but lead(II) ion is expected to be adaptable enough to such variation. Thus, we examined stepwise template reactions using lead(II) ion as the second template, and obtained macrocycles for a fairly wide range of the m,n set as trinuclear complexes, $[Pb(ML^{m,n})_2]X_2$ (M = Ni or Cu). The yields of the complexes are given in Table 1 together with analytical data.

When [*N,N'*-ethylenebis(3-formyl-5-methylsalicylideneiminato)]nickel(II) was adopted as a precursor complex the macrocycles $L^{2,3}$ and $L^{2,4}$ were obtained in tolerable yields. However, larger homologues with $n \geqslant 5$ were not obtained as the Ni_2Pb complexes. Macrocycles such as $L^{3,3}$ and $L^{3,4}$ could not be isolated as the Ni_2Pb complexes using [*N,N'*-propane-1,3-diylbis(3-formyl-5-methylsalicylideneiminato)]nickel(II) as a precursor complex.

It appears that the adoption of [*N,N'*-ethylene- and [*N,N'*-propane-1,3-diylbis(3-formyl-5-methylsalicylideneiminato)]-copper(II) as precursor complexes is suitable for the synthesis of $L^{m,n}$ of various m,n sets. Thus, $L^{2,5}$ and $L^{3,4}$ could be isolated as the Cu_2Pb complexes. The macrocycle $L^{2,2}$ could not be obtained as the M_2Pb complexes. This is probably because the second N_2O_2 cavity constructed with ethylenediamine is too small and rigid to incorporate a large lead(II) ion.

One might expect that the macrocycles $L^{m,n}$ can afford binuclear $[MPbL^{m,n}]^{2+}$ (M = Cu or Ni) complexes since binuclear lead(II) complexes $[Pb_2L^{3,3}]X_2$ (X = NO_3 or ClO_4)[13,19] have been obtained. However, we have not yet succeeded in obtaining such 1 : 1 type heteronuclear complexes.

Structure of $[Pb(CuL^{3,3})_2][ClO_4]_2$·dmf **10**.—An ORTEP view of the complex is shown in Fig. 2 along with the numbering scheme. Relevant bond distances and angles are given in Table 3.

The result demonstrates the formation of the macrocycle $L^{3,3}$. The crystal is comprised of the trinuclear complex cation $[Pb(CuL^{3,3})_2]^{2+}$, two perchlorate ions, and a dmf molecule. The perchlorate ions and the dmf molecule are free from co-ordination and captured in the crystal lattice. Two $CuL^{3,3}$ entities (macrocycles A and B) in the cation are structurally similar to each other, the copper(II) ion being bound at one of the N_2O_2 sites. The Cu–N and Cu–O bond distances fall in the range 1.91(1)–1.99(1) Å, slightly short compared with those of $[Cu_2L^{3,3}]Cl_2$ (Cu–N 1.978, Cu–O 1.981 Å).[20] It should be

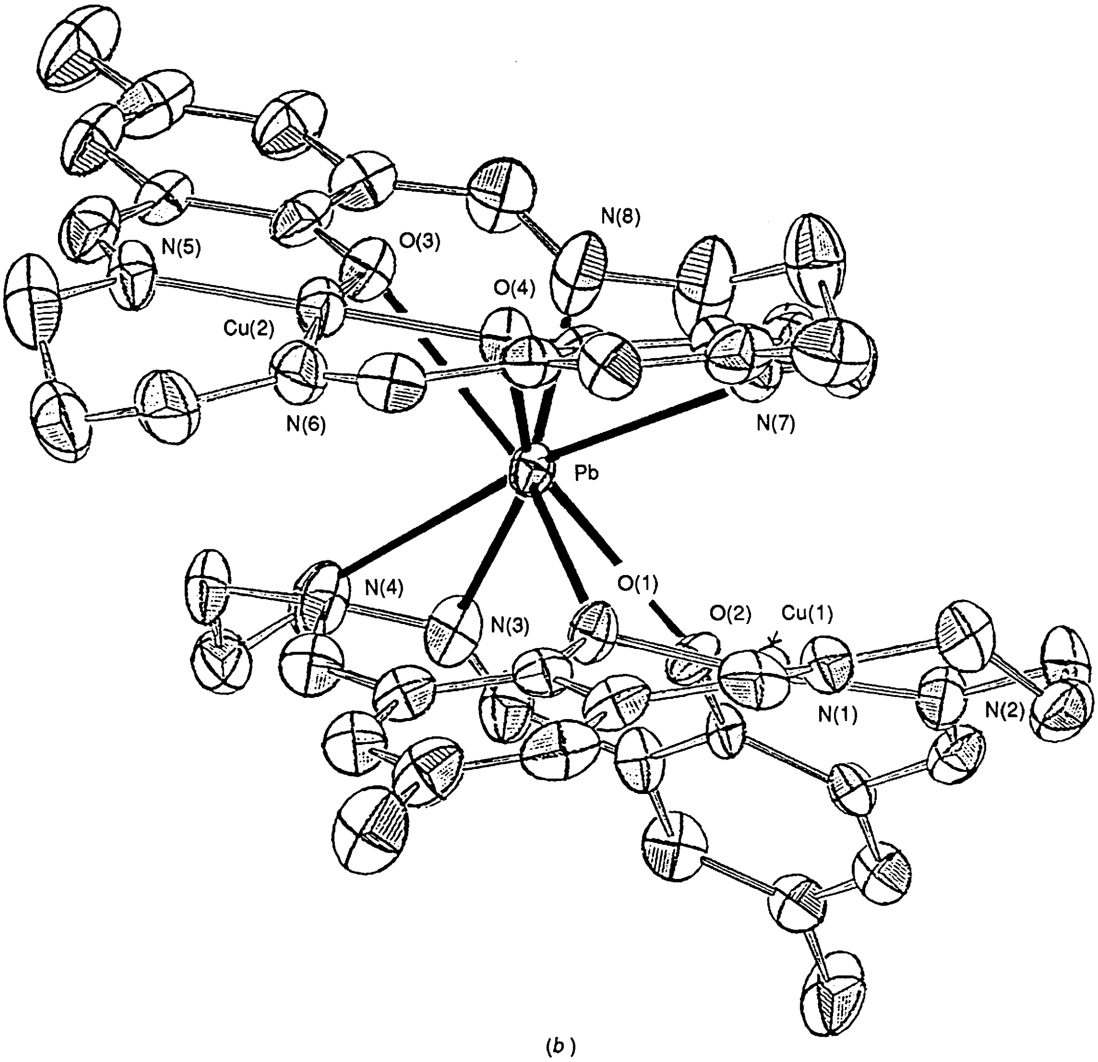

Fig. 2 ORTEP view of $[Pb(CuL^{3,3})_2][ClO_4]_2$·dmf: (*a*) a top view and (*b*) an edge view

noted that the Cu–N and Cu–O bond distances in these macrocyclic complexes are elongated compared with those of [*N*,*N*′-ethylenebis(salicylideneininato)]copper(II) (Cu–N 1.90–1.95, Cu–O 1.89–1.92 Å),[21] probably because of the bridging of the phenolic oxygens to the lead(II) ion. The other N_2O_2 site of $CuL^{3,3}$ is co-ordinated to the lead(II) ion. The lead(II) ion is sandwiched between two quadridentate $CuL^{3,3}$ molecules forming eight-co-ordination. The configuration around the Pb may be approximated by a square antiprism. The Cu(1)···Pb and Cu(2)···Pb separations are 3.442(2) and 3.424(2) Å, respectively. The Pb–N and Pb–O distances fall in the range 2.49(1)–2.71(1) Å, elongated compared with those of $[Pb_2L^{3,3}]^{2+}$ (2.36–2.48 Å),[19] probably because of the strong co-ordination of the phenolic oxygen to the copper(II) ion.

The weakened field strength of the second co-ordination site must be a reason why $ML^{m,n}$ (M = Cu or Ni) cannot form binuclear MPb complexes but trinuclear M_2Pb complexes. Recently, we have obtained CuPb complexes of macrocyclic analogues of those in Fig. 1(*a*), in which one lateral bridge is a simple alkane chain, $-(CH_2)_m-$ (m = 2 or 3), and another bridge is a hydroxyl-containing chain, $-(CH_2)_nCH(OH)(CH_2)_n-$ (n = 1 or 2).[22] In those CuPb complexes the second donor site of the macrocycles can incorporate a lead(II) ion by co-ordination of the hydroxy oxygen to the metal ion [Pb–O 2.61(2) Å]. Recently a macrocycle with two $-CH_2CH(OH)CH_2-$ lateral chains has been obtained by Tandon and McKee[23] as a Pb_2 complex. In this case also the donation of the hydroxy oxygen may contribute to the incorporation of a lead(II) ion into each co-ordination site.

General Characterization of the Complexes.—The FAB mass spectrum of complex **1** shows prominent signals at *m*/*z* 1199, 1100, 753, 654 and 447 which are reasonably assigned to $[Pb(NiL^{2,3})_2(ClO_4)]^+$, $[Pb(NiL^{2,3})_2]^+$, $[Pb(NiL^{2,3})(ClO_4)]^+$, $[PbNiL^{2,3}]^+$ and $[NiL^{2,3}]^+$, respectively. When the spectrum was expanded each signal was found to be comprised of several peaks. For example, that at *m*/*z* = 1199 is the strongest of a set of peaks from *m*/*z* = 1197 to 1203. The appearance of many peaks is due to the presence of isotopic atoms of both Ni and Pb (^{58}Ni, 67.76; ^{60}Ni, 26.16; ^{206}Pb, 25.15; ^{207}Pb, 21.7; ^{208}Pb, 52.3%).

The IR spectra of the complexes show no band attributable to the ν(N–H) and ν(C=O) vibrations. Instead a band attributable to ν(C=N) appears at 1620 cm^{-1}. Complexes **1**, **4** and **7**–**10** show an intense band at about 1100 cm^{-1} due to perchlorate vibration, indicating no co-ordination of this ion in accord with the X-ray result. Complexes **2** and **5** each shows an intense band at 840 cm^{-1} assigned to the hexafluorophosphate ion. Complex **6** shows a band at 1060 cm^{-1} due to tetrafluoroborate ion. The presence of tetraphenylborate ion in **3** and **11** is evidenced by the vibrations at 720 and 700 cm^{-1} characteristic of the phenyl group. The presence of acetonitrile in **3** is evidenced by a band at 2100 cm^{-1}, and the presence of dmf in **10** is evidenced by a band at 1645 cm^{-1}.

Electronic spectral data and magnetic moments at room temperature are summarized in Table 4. The Ni_2Pb complexes **1**–**6** are diamagnetic. They show two intense absorption bands at ≈325 and 402 nm in dmf which can be assigned to the π–π^* transition of the azomethine group and a charge-transfer

Table 3 Relevant bond distances (Å) and angles (°)

Co-ordination geometry around Pb

Pb $\cdots$ Cu(1)	3.442(2)	Pb $\cdots$ Cu(2)	3.424(2)
Pb–O(1)	2.49(1)	Pb–O(3)	2.67(1)
Pb–O(2)	2.65(1)	Pb–O(4)	2.56(1)
Pb–N(3)	2.71(1)	Pb–N(7)	2.63(1)
Pb–N(4)	2.68(1)	Pb–N(8)	2.69(2)
Cu(1)–Pb–Cu(2)	122.48(5)	N(3)–Pb–O(3)	110.7(3)
O(1)–Pb–O(2)	60.3(3)	N(3)–Pb–O(4)	155.0(3)
O(1)–Pb–N(3)	99.7(4)	N(3)–Pb–N(7)	134.9(4)
O(1)–Pb–N(4)	68.7(4)	N(3)–Pb–N(8)	93.0(4)
N(3)–Pb–N(4)	71.3(4)	N(4)–Pb–O(3)	81.3(3)
O(1)–Pb–O(3)	127.3(3)	N(4)–Pb–O(4)	84.8(4)
O(1)–Pb–O(4)	77.6(3)	N(4)–Pb–N(7)	144.1(4)
O(1)–Pb–N(7)	81.1(4)	N(4)–Pb–N(8)	137.1(4)
O(1)–Pb–N(8)	154.1(4)	O(3)–Pb–O(4)	56.8(3)
O(2)–Pb–N(3)	64.6(3)	O(3)–Pb–N(7)	103.6(3)
O(2)–Pb–N(4)	102.0(2)	O(3)–Pb–N(8)	67.0(4)
O(2)–Pb–O(3)	172.4(3)	N(7)–Pb–N(8)	74.0(4)
O(2)–Pb–O(4)	130.0(3)	O(4)–Pb–N(7)	69.8(3)
O(2)–Pb–N(7)	77.9(3)	O(4)–Pb–N(8)	100.0(4)
O(2)–Pb–N(8)	106.6(4)		

Co-ordination geometry around Cu

Cu(1)–O(1)	1.94(1)	Cu(2)–O(3)	1.91(1)
Cu(1)–O(2)	1.96(1)	Cu(2)–O(4)	1.94(1)
Cu(1)–N(1)	1.96(1)	Cu(2)–N(5)	1.99(1)
Cu(1)–N(2)	1.97(1)	Cu(2)–N(6)	1.95(2)
O(1)–Cu(1)–O(2)	82.8(4)	O(3)–Cu(2)–O(4)	80.7(4)
O(1)–Cu(1)–N(1)	91.2(5)	O(3)–Cu(2)–N(5)	90.2(5)
O(1)–Cu(1)–N(2)	171.0(5)	O(3)–Cu(2)–N(6)	169.3(6)
N(1)–Cu(1)–N(2)	95.8(6)	N(5)–Cu(2)–N(6)	98.4(6)
O(2)–Cu(1)–N(1)	171.3(5)	O(4)–Cu(2)–N(5)	170.7(5)
O(2)–Cu(1)–N(2)	89.6(5)	O(4)–Cu(2)–N(6)	90.5(5)

Table 4 Electronic spectral data and magnetic moments at room temperature for the complexes

Complex	λ_{max}/nm (ε/dm^3 mol^{-1} cm^{-1})	μ/μ_B
3	326 (8 500), 402 (7 900), 530(sh)	Diamagnetic
6	324 (8 900), 402 (7 600), 530(sh)	Diamagnetic
7	390 (9 400), 550 (160)	1.90
8	381 (9 800), 569 (170)	1.78
9	381 (10 000), 577 (175)	1.83
10	381 (10 600), 600 (65)	1.83
11	389 (10 900), 585 (90)	1.84

sh = Shoulder.

transition, respectively.[24] Both bands show a slight shift to lower energy relative to those of the precursor complex [*N*,*N*′-ethylenebis(salicylideneiminato)]nickel(II) and its homologues.[24] A d–d transition band of the nickel(II) ion appears as a discernible shoulder at 530 nm, practically the same wavelength as that of the precursor complex.[5]

The electronic spectra of the Cu_2Pb complexes **7–11** in dmf show the π–π^* transition at 380–390 nm[25] and a d–d transition at 550–600 nm. The π–π^* transition shifts to lower energy relative to that of the corresponding precursor complex.[25] The d–d band is located at nearly the same wavelength as that of the corresponding precursor complex. Because of the red shift of the π–π^* band all the Cu_2Pb complexes assume a brownish colour. The magnetic moments (per Cu) of the complexes fall in the range 1.78–1.90 μ_B which is common for magnetically isolated copper(II) complexes. Further, the magnetic moments were found to be practically independent of temperature down to liquid-nitrogen temperature, suggesting no pronounced magnetic interaction between the two copper(II) ions within a molecule. This is compatible with the X-ray structural result indicating a long Cu $\cdots$ Cu separation ($\approx$6.0 Å).

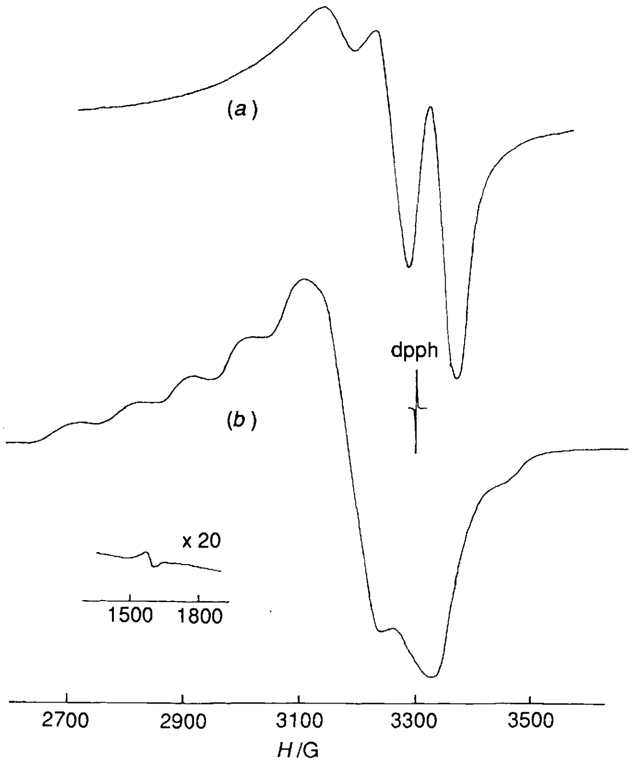

Fig. 3 ESR spectra of complex **1**: (*a*) dmf solution at room temperature and (*b*) frozen dmf solution at liquid-nitrogen temperature

The ESR spectra of complexes **7–11** measured in dmf at room temperature show an isotropic signal with a four-line hyperfine structure (g_{iso} = 2.10–2.11, A_{iso} = 80–85 G [see Fig. 3(*a*)]. Such ESR spectra are characteristic of magnetically diluted copper(II). When measured on frozen solutions at liquid-nitrogen temperature, the spectra bear an axial pattern but on the $g_{\parallel}$ component is superposed a multiline hyperfine structure [see Fig. 3(*b*)]. Further, the so-called half-field band is seen near 1600 G ($g \approx 4.1$). The hyperfine coupling constant (90–100 G) is about one half of that of monomeric copper(II) complexes[26] and comparible to that of the spin-triplet state of magnetically coupled dicopper(II) complexes.[27–29] This fact strongly suggests that the multiline structure arises from the spin-triplet state. It appears that [PbCuL^{m,n}] aggregates at low temperature through an out-of-plane interaction between CuN_2O_2 entities, as demonstrated for [*N*,*N*′-ethylenebis(salicylideneiminato)]copper(II) based on single-crystal X-ray analysis[30] and cryomagnetic[31] and ESR studies.[32] It is also noted that the multiline hyperfine structure (seven lines) is well resolved for complexes **7–9** whose CuN_2O_2 chromophore is formed with an ethylene chain (m = 2) whereas it is poorly resolved for **10** and **11** whose CuN_2O_2 chromophore is formed with a trimethylene chain (m = 3). In the latter complexes the spectral feature is evidently the superposition of a four-line structure (A = 190 G, major signal) and a seven-line structure (A = 95 G, minor signal), indicating that both monomeric and dimeric copper(II) species are coexisting. In those complexes the out-of-plane interaction must be difficult for steric reasons because the chelate ring constructed with the trimethylene chain assumes a chair conformation.[12,19]

References

1 P. K. Coughlin and S. J. Lippard, *J. Am. Chem. Soc.*, 1984, **106**, 2328; Y. Agnus, R. Louis, J.-P. Gisselbrecht and R. Weiss, *J. Am. Chem. Soc.*, 1984, **106**, 93.

2 J. M. Lehn, *Pure Appl. Chem.*, 1980, **52**, 2441; S. M. Nelson, *Pure Appl. Chem.*, 1980, **52**, 2461; D. E. Fenton, V. Casellato, P. A. Vigato and M. Vidali, *Inorg. Chim. Acta*, 1982, **62**, 57.

3 S. E. Groh, *Isr. J. Chem.*, 1976–1977, **15**, 277.

4 P. Zanello, S. Tamburini, P. A. Vigato and G. A. Mazzocchin, *Coord. Chem. Rev.*, 1987, **77**, 165.

5 N. H. Pilkington and R. Robson, *Aust. J. Chem.*, 1970, **23**, 2225.

6 H. Ōkawa and S. Kida, *Inorg. Nucl. Chem. Lett.*, 1971, **7**, 751; *Bull. Chem. Soc. Jpn.*, 1972, **45**, 1759.

7 A. W. Addison, *Inorg. Nucl. Chem. Lett.*, 1976, **12**, 899.

8 (*a*) R. R. Gagne, C. A. Koval and T. J. Smith, *J. Am. Chem. Soc.*, 1977, **99**, 8367; (*b*) R. R. Gagne, C. A. Koval, T. J. Smith and M. C. Cimolino, *J. Am. Chem. Soc.*, 1979, **101**, 4571; (*c*) R. R. Gagne, C. L. Spiro, T. J. Smith, C. A. Hamann, W. R. Thies and A. K. Shiemke, *J. Am. Chem. Soc.*, 1981, **103**, 4073; (*d*) C. L. Spiro, S. E. Lambert, T. J. Smith, E. N. Duesler, R. R. Gagne and D. N. Hendrickson, *Inorg. Chem.*, 1981, **20**, 1229.

9 (*a*) R. C. Long and D. N. Hendrickson, *J. Am. Chem. Soc.*, 1983, **105**, 1513; (*b*) S. L. Lambet and D. N. Hendrickson, *Inorg. Chem.*, 1979, **18**, 2683.

10 S. K. Mandal and K. Nag, *J. Chem. Soc., Dalton Trans.*, 1983, 2429.

11 S. K. Mandal and K. Nag, *J. Chem. Soc., Dalton Trans.*, 1984, 2141; S. K. Mandal, B. Adhikary and K. Nag, *J. Chem. Soc., Dalton Trans.*, 1986, 1175.

12 B. F. Hoskins, R. Robson and G. A. Williams, *Inorg. Chim. Acta*, 1976, **16**, 121; B. F. Hoskins and G. A. Williams, *Aust. J. Chem.*, 1975, **28**, 2593, 2607.

13 S. K. Mandal, L. K. Thompson, K. Nag and J.-P. Charland, *Inorg. Chem.*, 1987, **26**, 1391; S. K. Mandal, L. K. Thompson, K. Nag, J.-P. Charland and E. J. Gabe, *Can. J. Chem.*, 1987, **65**, 2815.

14 A. Denton and H. Suschitzky, *J. Chem. Soc.*, 1963, 4741.

15 A. T. C. North, D. C. Phillips and F. S. Mathews, *Acta Crystallogr., Sect. A*, 1968, **24**, 351.

16 *International Tables for X-Ray Crystallography*, Kynoch Press, Birmingham, 1974, vol. 4.

17 T. Sakurai and K. Kobayashi, *Rikagaku Kenkyusho Hokoku*, 1979, **55**, 69.

18 S. M. Nelson, *Pure Appl. Chem.*, 1980, **52**, 2461.

19 M. Tadokoro, H. Sakiyama, N. Matsumoto, H. Ōkawa and S. Kida, *Bull. Chem. Soc. Jpn.*, 1990, **63**, 3337.

20 B. F. Hoskins, N. J. McLeod and H. A. Schaap, *Aust. J. Chem.*, 1976, **29**, 515.

21 E. N. Baker, D. Hall and T. N. Waters, *J. Chem. Soc. A*, 1970, **400**, 406.

22 M. Tadokoro, H. Ōkawa, N. Matsumoto, M. Kodera and S. Kida, Symposium on Co-ordination Chemistry in Japan, Kanazawa, 1990.

23 S. S. Tandon and V. McKee, *J. Chem. Soc., Dalton Trans.*, 1989, 19.

24 B. Bosnich, *J. Am. Chem. Soc.*, 1968, **90**, 627.

25 R. S. Downing and F. L. Urbach, *J. Am. Chem. Soc.*, 1969, **91**, 5977.

26 Y. Nonaka, T. Tokii and S. Kida, *Bull. Chem. Soc. Jpn.*, 1974, **47**, 312.

27 G. F. Kokoszka, M. Linzer and G. Gordon, *Inorg. Chem.*, 1968, **7**, 1730.

28 R. W. Duerst, S. J. Baum and G. F. Kokoszka, *Nature* (*London*), 1969, **222**, 665.

29 T. Kamiusuki, H. Ōkawa, E. Kitaura, M. Koikawa, H. Matsumoto, H. Oshio and S. Kida, *J. Chem. Soc., Dalton Trans.*, 1989, 2077.

30 D. Hall and T. N. Waters, *J. Chem. Soc.*, 1960, 2644.

31 M. Calvin and C. H. Barkelew, *J. Am. Chem. Soc.*, 1946, **68**, 2267.

32 G. O. Carisle and W. E. Hatfield, *Inorg. Nucl. Chem. Lett.*, 1970, **6**, 633.

Received 12*th November* 1990; *Paper* 0/05089J